

Article

Light-Activated Modified Arginine Carbon Dots as Antibacterial Particles

Selin S. Suner ¹, Mehtap Sahiner ², Aynur S. Yilmaz ¹, Ramesh S. Ayyala ³ and Nurettin Sahiner ^{1,3,4,*}

¹ Department of Chemistry, Faculty of Sciences & Arts, Nanoscience and Technology Research and Application Center (NANORAC), Canakkale Onsekiz Mart University Terzioğlu Campus, Canakkale 17100, Turkey

² Department of Bioengineering, Faculty of Engineering, Canakkale Onsekiz Mart University Terzioğlu Campus, Canakkale 17100, Turkey

³ Department of Ophthalmology, Morsani College of Medicine, University of South Florida Eye Institute, Tampa, FL 33612, USA

⁴ Department of Chemical & Biomedical Engineering, Materials Science and Engineering Program, University of South Florida, Tampa, FL 33620, USA

* Correspondence: sahin71@gmail.com or nsahiner@usf.edu

Abstract: Nitrogen-doped arginine carbon dots (Arg CDs) as light-sensitive antibacterial agents were prepared by using citric acid as the carbon source and arginine amino acid as the nitrogen source via a microwave-assisted synthesis method. Dynamic light scattering (DLS) measurements and TEM images revealed that the Arg CDs were in the 1–10 nm size range with a graphitic structure. To improve their antibacterial capability, the Arg CDs were modified with ethyleneimine (EDA), pentaethylenehexamine (PEHA), and polyethyleneimine (PEI) as different amine sources, and the zeta potential value of $+2.8 \pm 0.6$ mV for Arg CDs was increased to $+34.4 \pm 4.1$ mV for PEI-modified Arg CDs. The fluorescence intensity of the Arg CDs was significantly enhanced after the modification with EDA, and the highest antibacterial effect was observed for the PEI-modified Arg CDs. Furthermore, the photodynamic antibacterial capacity of bare and EDA-modified Arg CDs was determined upon light exposure to show their light-induced antibacterial effects. Photoexcited (315–400 nm, UVA, 300 W), EDA-modified Arg CDs at 5 mg/mL concentration were found to inhibit about $49 \pm 7\%$ of pathogenic bacteria, e.g., *Escherichia coli*, with 5 min of light exposure. Furthermore, the biocompatibilities of the bare and modified Arg CDs were also investigated with blood compatibility tests via hemolysis and blood clotting assays and cytotoxicity analysis on L929 fibroblast cells.



Citation: Suner, S.S.; Sahiner, M.; Yilmaz, A.S.; Ayyala, R.S.; Sahiner, N. Light-Activated Modified Arginine Carbon Dots as Antibacterial Particles. *Catalysts* **2022**, *12*, 1376. <https://doi.org/10.3390/catal12111376>

Academic Editors:
Roberto Comparelli and Ilaria De Pasquale

Received: 5 October 2022

Accepted: 4 November 2022

Published: 7 November 2022

Publisher's Note: MDPI stays neutral with regard to jurisdictional claims in published maps and institutional affiliations.



Copyright: © 2022 by the authors. Licensee MDPI, Basel, Switzerland. This article is an open access article distributed under the terms and conditions of the Creative Commons Attribution (CC BY) license (<https://creativecommons.org/licenses/by/4.0/>).

Keywords: arginine; carbon dots; modified carbon dots; photodynamic antibacterial; UV light

1. Introduction

Carbon dots (CDs), also referred to as graphene carbon dots, are carbon-based materials with a size of less than 20 nm [1]. Graphene dots, amorphous carbon dots, and polymer-like dots are subgroups of CDs [2]. They can be fabricated through solvothermal/hydrothermal reactions [3], laser ablation [4], ultrasonic-assisted synthesis [5], electrochemical etching [6], and more commonly microwave treatments [7,8] involving natural and synthetic precursor strategies [2]. The unique properties of CDs, including dispersibility, water solubility, low toxicity, excellent optical properties such as fluorescence properties, cheap and facile synthesis, and environmental friendliness, make them promising materials in biomedical applications [9]. CDs have been used in various application fields in bioimaging [10], biosensors [11], bioconjugation [12], drug carriers [13], gene delivery [14], fluorescent labeling or probes [11], cancer theragnostics [15], and so on [16]. For biological applications, CDs' toxicity can be further diminished by using biocompatible precursor molecules such as amino acids [17,18], carbohydrates [19], etc., and amino-acid-modified CDs could provide improved surface functions as well as new applications, e.g., drug delivery [2]. In particular, natural-based and nitrogen-/sulfur-doped CDs have attracted

much attention in biomedical use because of their inherent antimicrobial and antibiofilm activities [20] as well as innate biocompatibilities [11]. Due to their broad optical spectral coverage and other remarkable properties, CDs can act as photosensitizer nanomaterials under UV–visible light [21,22], Xe lamp [23], blue light [24,25], and NIR lights [26]. Meziani et al. reported that the optical absorption of CDs is related to the π -plasmon transition in the core of nanoparticles with a broad and strong absorption spectrum in the visible region [27]. The photoexcited behavior of CDs is substantially attributed to the separation of photoinduced radical anions and cations as electrons and holes, and their radiative recombination in bright and multicolored fluorescence emissions [28–30]. Light exposure can excite an electron from the valence band to the conduction band, leaving a positive hole in its place because of the confinement of electrons. Photoexcitation results in the generation of reactive oxygen species (ROS) produced via energy or electron transfer to molecular oxygen [31,32]. As a result, readily generated free radicals, reactive oxygen species, and ROS-dependent lipid peroxidation damages cellular membranes in living organisms [31]. Due to the accumulative nature of ROS in cells and photoexcited redox characteristics, natural antioxidants fail in neutralizing this damage resulting in a collapse of cellular functions [33]. Photodynamic inactivation of bacteria mediated by photoactive compounds, or rather photosensitizing molecules, is one of the most promising techniques, and CDs are candidate nanomaterials as photodynamic therapy agents in the fight against pathogens [27,34]. In comparison to the conventional strategies, CDs have important advantages, i.e., minimal invasiveness, less side effects, less likely to trigger antimicrobial resistance of targeted microorganisms [35], non-toxicity [36], and exceptional fluorescence and photostability [34]. Quantum yields, surface charge and thus binding-like interactions [37], and oxygen functionalization are responsible for these photodynamic activities in CDs [27,30] and can be designed or modified as such depending on the requirements.

In this study, N-doped CDs were prepared as a photosensitive antibacterial biomaterial using arginine (Arg) and citric acid via a microwave-assisted method within just 2 min. Due to comprising well-organized carbon atoms and abundant functional groups, the CDs were functionalized by different modifying agents with a high adsorption capacity, high thermal and chemical stability, large surface area, and significantly higher drug-loading capacity [38,39]. Thus, to improve the antibacterial activity of Arg CDs, three different amine sources—ethyleneimine (EDA), pentaethylenhexamine (PEHA), and polyethyleneimine (PEI)—were reacted with the Arg CDs as modifying agents. The size distribution, morphologic structure, surface character, and optical properties of these CDs were measured by DLS, TEM images, zeta potential measurements, and UV–vis and fluorescence spectroscopies. The hemolytic activity and biocompatibility of the Arg CDs and their amine-modified forms were investigated by blood compatibility tests such as hemolysis and blood clotting index assays and cytotoxicity analysis on L929 fibroblast cells. The minimum inhibition concentration values of the Arg-based CDs were evaluated by microtiter broth dilution methods to determine their antibacterial effects. Furthermore, the photodynamic, antibacterial susceptibility of the Arg CDs and modified Arg CDs by ROS activity was investigated under UV light irradiation with up to 30 min light exposure.

2. Results and Discussion

The Arg CDs were prepared by a microwave synthesis method within 2 min in a single-step reaction of citric acid and arginine amino acid in accordance with our previously reported study [40,41]. The morphological structure of the Arg CDs was visualized by TEM images, and the corresponding image are shown in Figure 1a. Spherical-shaped Arg CDs were successfully prepared with a size of less than 10 nm. Similarly, DLS measurement of the Arg CDs revealed that the hydrodynamic size distribution was changed between 0.5 nm and 10 nm with nearly a 2.3 ± 0.8 nm average size, as demonstrated in Figure 1b. Furthermore, the particle size distribution and crystalline structure of the Arg CDs were determined with HR-TEM images.

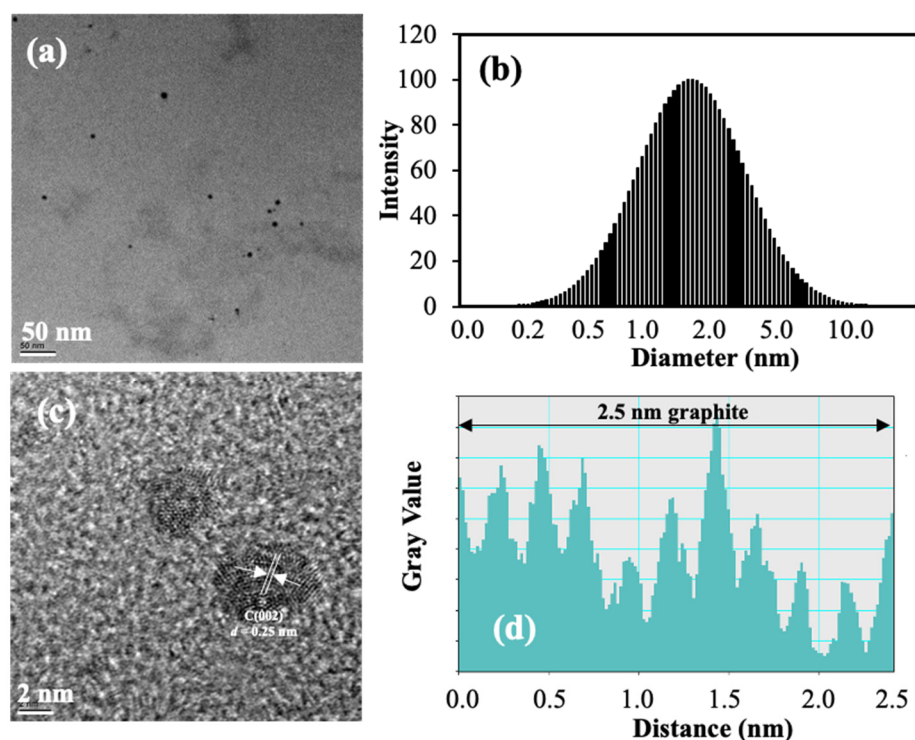


Figure 1. (a) TEM images of Arg CDs and (b) their particle size distribution by DLS measurements; (c) HR-TEM images of Arg CDs and (d) the corresponding gray value plot.

As indicated in Figure 1c,d, the size of the Arg CDs is measured to be from 2 nm to 5 nm, which is similar to the DLS results, and a graphitic structure was observed with a 0.25 nm lattice space of the CDs. The Arg CDs were reacted with three different modifying agents with different numbers of amine groups such as EDA, PEHA, and PEI to prepare amine-modified Arg CDs. The reaction mechanism and chemical structure of these modifying agents and their reactions are represented in Figure 2a. The Arg CDs were reacted with an ECH coupling agent in a basic condition before the modification reactions. Deprotonated hydroxyl and amine groups of Arg CDs can readily react with ECH on CDs. Then, EDA, PEHA, or PEI was added in the reaction medium as an amine source. These modifying agents can react with the epoxide ring of the ECH coupling agent at 50 °C. These modifying agents have different sizes and structures and have different numbers of amine groups. The chemical structure of the Arg CDs and their modified forms were assessed by FT-IR analysis as illustrated in Figure 2b. From the FT-IR spectra, the intensity of the broad band in the 3500–3000 cm^{-1} range and the peaks at 2955 and 2877 cm^{-1} due to stretching vibrations of the $-\text{NH}_2$ and $-\text{CH}_2$ groups were significantly increased upon the modification reactions because of the presence of the amine groups of the modifying agents. Similarly, the intensities of 1458 cm^{-1} and 1057 cm^{-1} attributed to the C-H [42] and C-N groups belonging to the modifying agents at the surface of the Arg CDs were increased. In particular, the peak at 1578 cm^{-1} was clearly present in the Arg-PEI CDs coming from the N-H groups of PEI.

In addition to the FT-IR results, the zeta potential values of bare and modified Arg CDs were also measured to determine the change in the surface zeta potential values of the modified Arg CDs. As summarized in Table 1, the zeta potential value of the Arg CDs was measured as $+2.77 \pm 0.51$ mV.

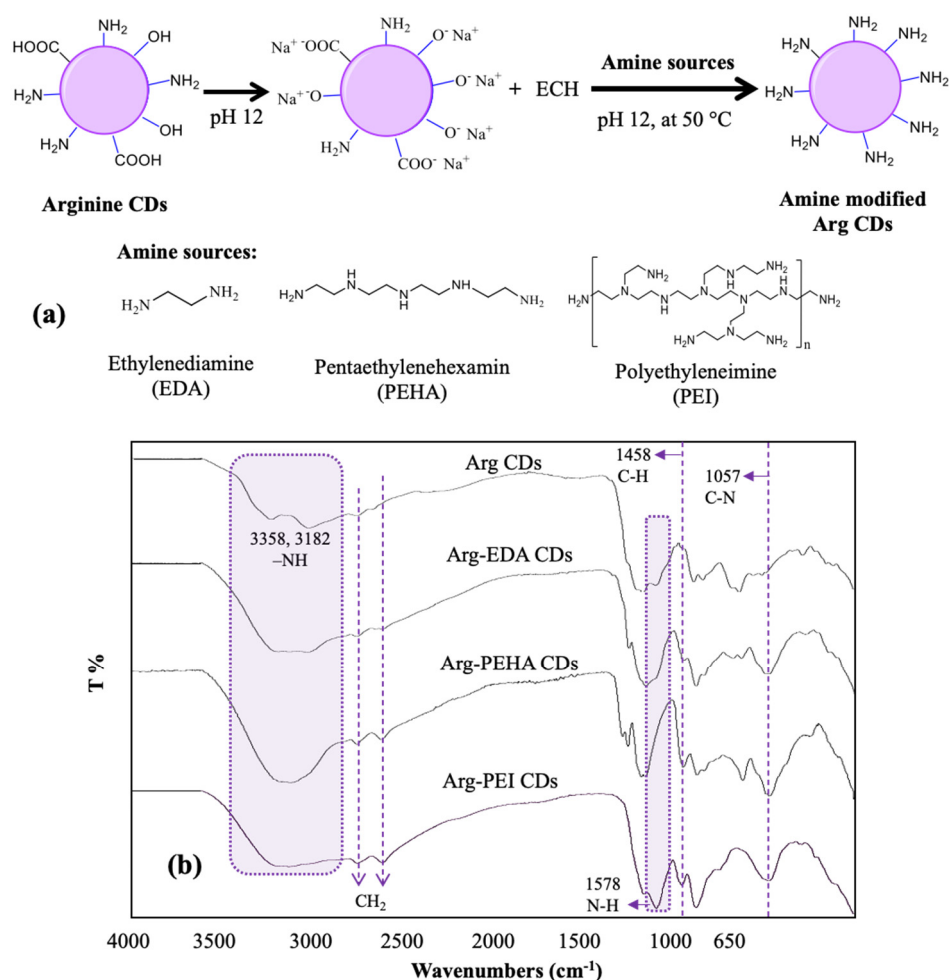


Figure 2. (a) Schematic representation of modification reaction of arginine CDs with different amine sources such as ethylenediamine (EDA), triethylenetetramine (TETA), pentaethylenhexamine (PEHA), and polyethyleneimine (PEI), and (b) FT-IR spectrum of arginine CDs and modified arginine-PEI CDs.

Table 1. Zeta potential values of arginine CDs and its amine-modified forms with different amine sources.

Carbon Dots	Zeta Potential (mV)
Arg	+2.77 ± 0.51
Arg-EDA	+19.46 ± 1.48
Arg-PEHA	+22.34 ± 4.59
Arg-PEI	+34.41 ± 4.17

On the other hand, the amine-modified Arg-EDA, Arg-PEHA, and Arg-PEI CDs revealed a more cationic structure than the Arg CDs, and zeta potential values of +19.46 ± 1.48, +22.34 ± 4.59, and +34.41 ± 14.17 mV, respectively, were measured. The FT-IR spectra and zeta potential results supported that almost all functional groups of the Arg CDs were turned to -NH₂ groups, and different numbers and forms of amine sources were used to coat the surface of the Arg CDs.

The optical properties of Arg-based CDs were evaluated by UV-vis and fluorescence spectroscopies, and the corresponding spectra are presented in Figure 3a,b, respectively.

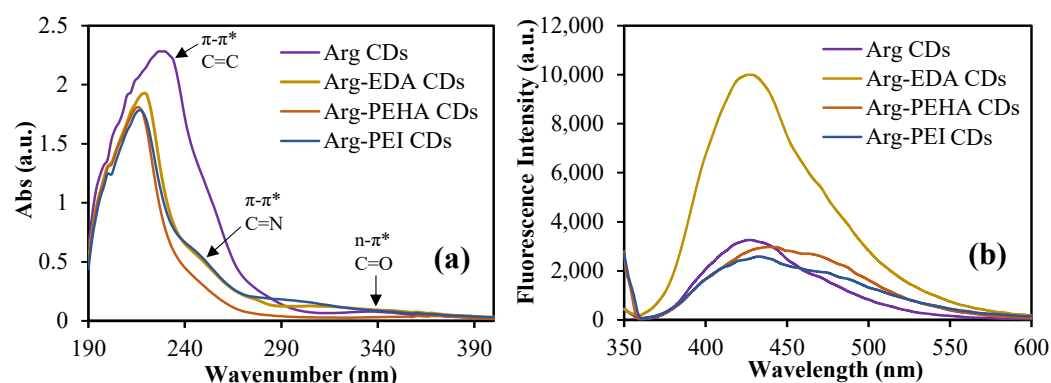


Figure 3. (a) UV-vis absorption spectra and (b) fluorescence emission spectra of amino-acid-derived CDs (excitation at 345 nm).

In the UV-vis spectra, there is a high absorption peak at 230 nm assigned to the π - π^* electron transition of C=C which can be observed for all forms of CDs [40]. Only Arg CDs show a low absorption band at 340 nm, which is attributed to the n - π^* transition of C=O because of free surface functional groups of Arg CDs before the amine modification reaction [21]. In addition, the absorption bands at about 250 nm were observed, especially for modified Arg CDs coming from the π - π^* transition of C=N groups [41]. In the fluorescence properties, the suspension of Arg-based CDs in DI water was measured at the 345 nm excitation wavelength, and the maximum emission was represented at about 430 nm. Furthermore, the fluorescence intensity was almost the same for Arg, Arg-PEHA, and Arg-PEI CDs, but significantly increased, i.e., by almost three-fold, for Arg-EDA CDs.

The blood compatibility of Arg-based CDs was determined by hemolysis and blood clotting index tests, and the results are demonstrated in Figure 4a,b, respectively.

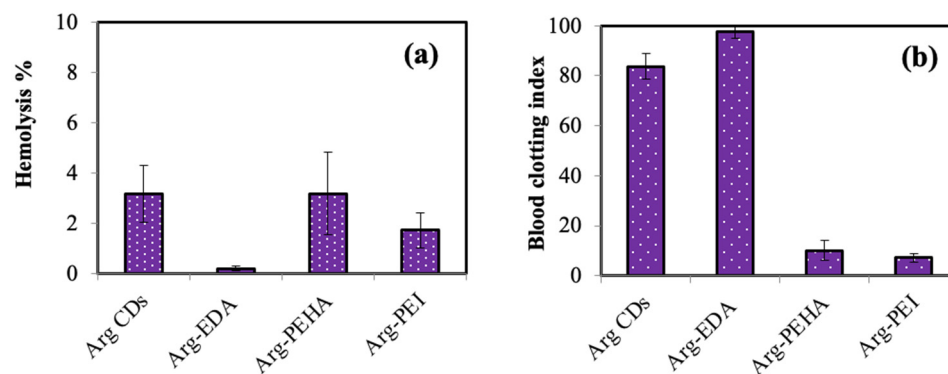


Figure 4. (a) Hemolysis % and (b) blood clotting indexes of Arg CDs and their modified forms at 250 μ g/mL concentration.

Hemolysis % shows the blood toxicity of the materials on erythrocyte cells which are known as red blood cells. The materials should exhibit a maximum of 5% hemolysis to be considered blood compatible for intravenous application. The hemolysis % of the Arg, Arg-EDA, Arg-PEHA, and Arg-PEI CDs at 0.25 mg/mL concentration was found to be 3.15 ± 0.78 , 0.2 ± 0.11 , 3.17 ± 1.03 , and $1.71 \pm 0.42\%$, respectively. Arg CDs and Arg-PEHA CDs had slightly hemolytic biomaterials with a 2–5% hemolysis ratio, but Arg-EDA and Arg-PEI CDs were found to be non-hemolytic with a <2% hemolysis value. These results indicated that all types of Arg-based CDs are not toxic, do not significantly destroy the erythrocyte cells, and could be used in blood-contacting intravenous applications accordingly. The other blood compatibility test was the blood clotting index that is related to the clotting mechanism of the blood-contacting materials. The blood clotting index values of the Arg, Arg-EDA, Arg-PEHA, and Arg-PEI CDs at 0.25 mg/mL concentration were measured as 83.8 ± 2.1 , 97.5 ± 0.3 , 10.2 ± 1.03 , and $7.2 \pm 0.1\%$, respectively. Therefore,

it can be assumed that Arg CDs and Arg-EDA CDs were blood-compatible materials due to the high blood clotting values which had no significant effects on the blood clotting mechanism. In addition, Arg-PEHA and Arg-PEI CDs can clot the blood within 10 min with very low blood clotting index values and are safely used in intravenous applications. Moreover, these Arg-PEHA and Arg-PEI CDs could be used as coagulation agents, which are also very important to stop bleeding in certain injuries.

The cytotoxicity of Arg-based CDs in the 50 to 1000 µg/mL concentration range was investigated on L929 fibroblast cells for a 24 h incubation time via an MTT assay.

As seen in Figure 5, the viability of the fibroblast cell was decreased to 68% for Arg CDs at 50 µg/mL concentration, but modified Arg-EDA, Arg-PEHA, and Arg-PEI CDs at the same concentration did not significantly affect the fibroblast viability. The experimental results demonstrated that the toxicity limit of the Arg-based CDs is about 100 µg/mL concentration as cell viability values of more than 60% were attained below this concentration for the materials. CDs can also be combined with particular antimicrobial agents as carriers e.g., with antibiotics that are toxic when used alone, and therefore, the toxicity from these toxic antimicrobial chemicals can be minimized contributing greatly to the reduction in antimicrobial resistance development [43]. Our results showed that more toxic amine sources could be used on the surface of the CDs at a certain concentration without causing significant toxicity.

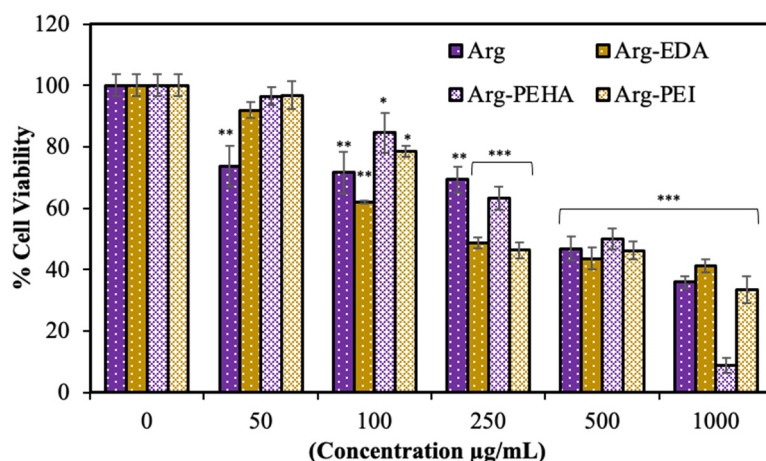


Figure 5. Cytotoxicity of Arg CDs and their modified forms, Arg-EDA, Arg-PEHA, and Arg-PEI CDs, on L929 fibroblast cells for 24 h incubation time [$* p < 0.05$, $** p < 0.01$, $*** p < 0.001$ vs. control].

The antimicrobial properties of the Arg, Arg-EDA, Arg-PEHA, and Arg-PEI CDs were investigated against gram-negative *E. coli* and gram-positive *S. aureus* bacteria strains by microtiter tests. The results of the minimum inhibition concentration (MIC, mg/mL) values of Arg-based CDs are given in Figure 6. The MIC value of Arg CDs was found to be 3.12 mg/mL against both *E. coli* and *S. aureus* species. The MIC values of Arg-EDA and Arg-PEHA CDs were not changed against *S. aureus*; however, a two-fold decrease against *E. coli*, with a 1.75 mg/mL MIC value, was observed. These results indicate that Arg-EDA and Arg-PEHA CDs have almost the same antibacterial effects on gram-negative and gram-positive bacteria strains because they have almost the same zeta potential values. Among these materials, the highest antibacterial ability was obtained for Arg-PEI CDs against both bacteria, with a very low MIC value of 0.2 mg/mL.

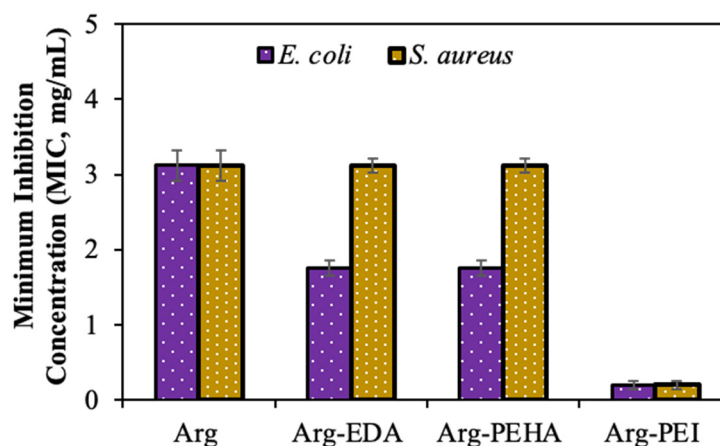


Figure 6. Minimum inhibition concentration (MIC) of Arg, Arg-EDA, Arg-PEHA, Arg-PEI CDs against *E. coli* ATCC 8739 (gram -) and *S. aureus* ATCC 6538 (gram +) for 24 h incubation time.

These results demonstrated that branched amine sources such as PEI is the most effective modifying agent for Arg CDs on the model pathogenic bacteria strains. Dong et al. reported that a combination of CDs with certain antimicrobial reagents have a synergistic effect in inhibiting bacterial growth [43]. Similarly, the inherent antibacterial activity of Arg CDs can be significantly improved by a modification reaction with different amine sources.

CDs are attracting increased attention as photoinduced antibacterial nanomaterials in photodynamic therapy. It is well known that because of the excellent optical properties of CDs, especially fluorescence properties, they can create reactive oxygen species (ROS) under light exposure that can cause significant damage to the DNA or membrane structure of microorganism species and can inhibit pathogen growth [21]. For analysis, concentrations of 1, 5, and 10 mg/mL of the Arg CDs and modified CDs—Arg-EDA, Arg-PEHA, and Arg-PEI CDs were interacted with *E. coli* suspension in 0.9% NaCl solution as a model pathogen and compared with the control group of just *E. coli* suspension in 0.9% NaCl solution (as 0 mg/mL particle concentration). These suspensions were placed in a dark environment or under UV light irradiation for 5 min or 30 min. The bacterial cell viability % at the end of the 5 and 30 min period for both Arg CDs under dark and/or light exposure are given in Figure 7. According to the results, in the experiment carried out in a dark environment, no significant inhibition was detected even after 30 min, except for the modified Arg-PEI CDs with almost half of the bacterial inhibition at 10 mg/mL concentration observed, as shown in Figure 7a,b. In the microtiter test, the MIC values of the Arg-based CDs were found below 10 mg/mL concentration for the 24 h incubation time, and the Arg-PEI CDs exhibited the highest antibacterial effect against *E. coli*. It could be assumed that the high bacteria concentration and low incubation time of only 30 min was not enough to inhibit the growth of *E. coli*, but only Arg-PEI CDs could kill the bacteria within 5 min in the photodynamic activity test without light exposure even in the dark condition. On the other hand, the Arg, Arg-EDA, Arg-PEHA, and Arg-PEI CDs with a 5 min UV light exposure had almost the same bacterial viability of $55 \pm 2\%$, $51 \pm 3\%$, $51 \pm 2\%$, and $65 \pm 3\%$ at a 5 mg/mL concentration, as shown in Figure 7c. As presented in Figure 7d, when the UV light irradiation time was increased to 30 min, only a 1 mg/mL concentration of Arg, Arg-EDA, Arg-PEHA, and Arg-PEI CDs provided $53 \pm 7\%$, $22 \pm 4\%$, $55 \pm 5\%$, and $51 \pm 5\%$ bacterial viability, respectively.

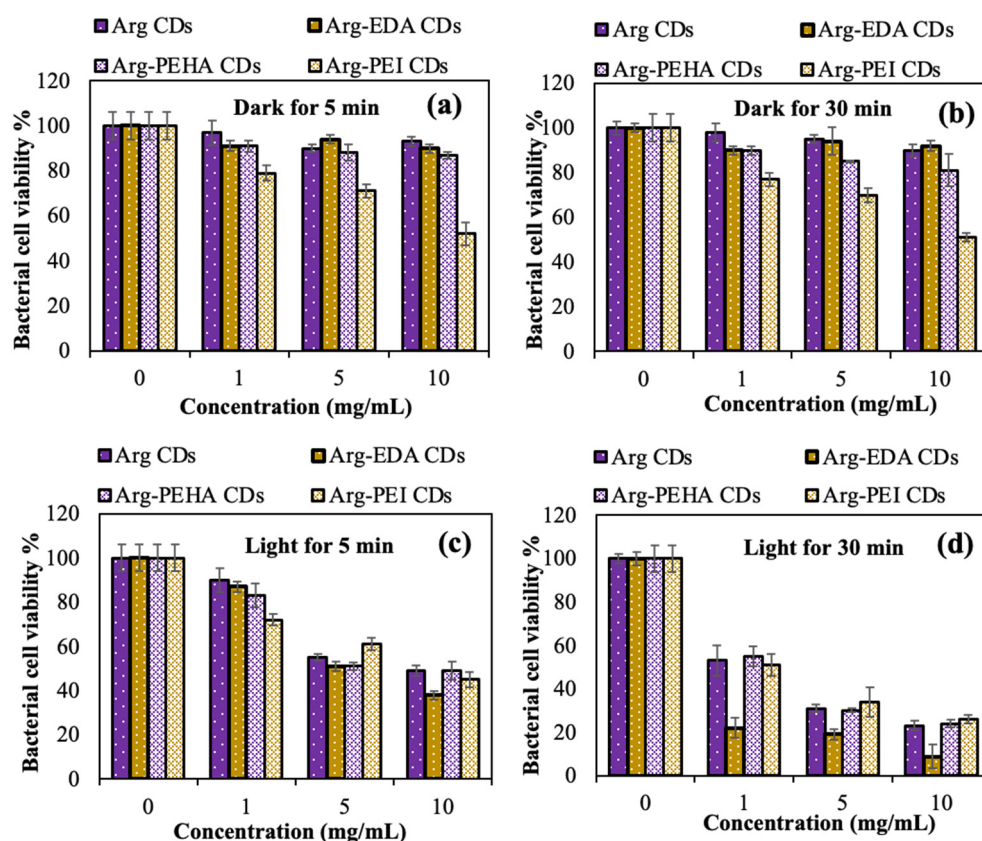


Figure 7. Photodynamic antibacterial activity of 1, 5, and 10 mg/mL concentrations of Arg, Arg-EDA, Arg-PEHA, and Arg-PEI CDs under dark conditions for (a) 5 min and (b) 30 min, and UV light irradiation for (c) 5 min and (d) 30 min against *E. coli* (gram -).

The difference in the inhibition % values of bacterial growth for Arg-PEI CDs before and after light exposure is not significant. Arg-EDA CDs exhibit the highest photoinduced inhibition with almost total inhibition at a 10 mg/mL concentration for 30 min of UV light exposure. Nichols and Chen indicated that the amount of ROS production was correlated with the fluorescent intensity of photoinduced materials [44]. Arg-based CDs are affected by light-induced bacterial growth inhibition, but modified Arg-EDA CDs resulted in higher photodynamic antibacterial activity inhibition than the bare and the other modified Arg CDs. The higher photodynamic activity of modified Arg-EDA CDs seems to be dependent on their having the highest fluorescence intensity in comparison to Arg-based CDs at the same concentration because the fluorescent property can afford improved ROS production as a killing agent for pathogens.

3. Materials and Methods

3.1. Materials

L-Arginine (Arg, >98%, Sigma-Aldrich, St. Louis, MO, USA) and citric acid monohydrate (CA, >99%, Carlo Erba, Val-de-Reuil, France) were purchased and used as received for synthesis of Arg CDs. In the modification reaction, sodium hydroxide (NaOH, 98%), epichlorohydrin (ECH >99%), ethylenediamine (EDA, 99.5%), triethylenetetramine (TETA, ≥97%), pentaethylenhexamine (PEHA, Technical grade), and polyethyleneimine (PEI, 50 wt%, Mn:1200) were obtained from Sigma-Aldrich. In the cytotoxicity test, the L929 fibroblast cell line was obtained from the SAP Institute, Ankara, Turkey. The cell culture medium, Dulbecco's modified Eagle's medium (DMEM/F-12, 1:1) (L-Glutamine, 15 mM HEPES, 1.2 g/L NaHCO₃), was purchased from Pan Biontech GmbH, Aidenbach, Germany. The fetal bovine serum (FBS), trypsin-EDTA (0.25%) and antibiotics (10,000 U/mL penicillin, 10,000 µg/mL streptomycin) were purchased from Pan Biontech GmbH, Aidenbach,

Germany. Trypan Blue (0.5% solution) was obtained from Biological Industries, and thiazolyl blue tetrazolium bromide (MTT) was acquired from BioFroxx (Einhausen, Germany). Dimethyl sulfoxide (DMSO, 99.9%) was obtained from Carlo-Erba. Gram-negative *Escherichia coli* ATCC 8739 and gram-positive *Staphylococcus aureus* ATCC 6538 were obtained from KWIK-STIK, Microbiologics. Nutrient agar (NA, Condolab, Madrid, Spain) as a solid growth medium and nutrient broth (NB, Merck, Darmstadt, Germany) as a liquid medium were purchased from and used as received. Acetone and ethanol were used as received and aqueous solutions were prepared with ultrapure water of nearly 18.2 M.Ω.cm obtained from a Millipore-Direct Q UV3 (Bedford, MA, USA).

3.2. Preparation of Arg CDs and Modified Arg CDs

Citric acid (CA) and arginine were reacted through a microwave-assisted method based on the procedure proposed by Suner et al. [41]. Briefly, 0.3 g of Arg and 0.6 g of CA were dissolved into 3 mL of DI water and stirred at 300 rpm for 15 min. Then, this Arg: CA solution was placed into a commercial microwave operating at 1000 W for 2 min. Carbonized Arg CDs were immediately suspended in 1 mL of DI water and sonicated for 10 sec to obtain the dispersion of the obtained CDs. Next, the Arg CDs were filtered with a 0.22 μm pore filter and placed into a dialysis membrane. Then, the dialysis membrane containing the Arg CDs was put into 200 mL of DI water, and the water was refreshed at least 5 times for the dialysis of CDs for 24 h. The Arg CD solution inside the membrane was precipitated by the addition of an excess amount of acetone, and the precipitated Arg CDs were washed with acetone by centrifugation process at 10,000 rpm for 10 min three times. The purified Arg CDs were dried in an oven at 50 °C and placed into a closed container for further use.

Amine modification of Arg CDs occurs through the reaction with ethyleneimine (EDA), pentaethylenehexamine (PEHA), or polyethyleneimine (PEI) amine sources by using a coupling agent, epichlorohydrin. For the modification reactions, 0.5 g of Arg CDs was suspended in 10 mL of pH 12 aqueous solution with NaOH. After mixing for 10 min at 300 rpm, 1 mL of ECH was added to the Arg suspension and stirred at the same condition for 1 h. Then, 1 mL of EDA, PEHA, or PEI was slowly added into the reaction medium and stirred at 50 °C for 1 h. The prepared EDA-, PEHA-, or PEI-modified Arg CDs were precipitated in 200 mL of acetone, and the precipitated CDs were washed with acetone by centrifugation process at 10,000 rpm for 10 min three times. The purified, modified Arg CDs were dried in an oven at 50 °C and placed into a closed container for further use.

3.3. Characterization of Arg-Based CDs

A high-resolution transmission electron microscope (HR-TEM, Tecnai TF-20, FEI Company, Osaka, Japan) was used to determine the size and crystal structure of Arg CDs. The images were taken at 200 kV after placing the samples on lacey carbon support film on a 200–300 mesh copper TEM grid. Hydrodynamic size distribution of the Arg CDs was determined by dynamic light scattering measurement (DLS, Nanobrook Omni Brookhaven Instrument, Holtsville, NY, USA). Briefly, 1 mg/mL of Arg CDs in 0.01 mol KNO₃ aqueous solution was measured by DLS. Similarly, 1 mg/mL of Arg-based CDs in 0.01 mol KNO₃ aqueous solution was measured with a zeta potential analyzer (Nanobrook Omni Brookhaven Instrument, Holtsville, NY, USA). All DLS and zeta measurements were repeated five times and the average values with standard deviations were presented. The chemical structure of Arg-based CDs was evaluated by FT-IR spectroscopic analysis (Perkin Elmer, Waltham, MA, USA) in the 650 to 4000 cm⁻¹ range using the ATR technique. In addition, the optical properties of Arg-based CDs were analyzed with a UV-vis spectrophotometer (T80 + UV/vis spectrometer, PG Instrument, Lutterworth, UK) and fluorescence spectrophotometer (Lumina, Thermo Scientific, Waltham, MA, USA). Fluorescence analysis was carried out at 345 nm excitation wavelength for a 350–600 nm emission wavelength range.

3.4. Blood Compatibility of Arg-Based CDs by Hemolysis and Blood Clotting Tests

To determine the blood compatibility of Arg-based CDs by hemolysis and blood clotting tests, an ethics committee approval was obtained from the Human Research Ethics Committee of Canakkale Onsekiz Mart University (2011-KAEK-27/2022), and the tests were performed accordingly. The fresh blood was taken from healthy volunteers and immediately placed into EDTA-containing hemogram tubes.

In the hemolysis analysis, 250 µg/mL concentration of Arg-based CDs was prepared in 10 mL of 0.9% NaCl solution and incubated at 37 °C in a shaking water bath. The blood in the hemogram tube was diluted with 0.9% NaCl solution to a 1:1.25 mL volume of blood: NaCl solution. Then, 0.2 mL of diluted blood was added onto the Arg suspension and incubated for 1 h at 37 °C in a shaking water bath. After that, the suspension was centrifuged at 100× g for 5 min, and the supernatant of this solution was measured with a UV-vis spectrophotometer at 542 nm. The hemolysis ratio % of the CDs was determined according to Equation (1):

$$\text{Hemolysis ratio}\% = (A_{\text{SAMPLE}} - A_{\text{NC}})/(A_{\text{PC}} - A_{\text{NC}}) \times 100 \quad (1)$$

where A_{SAMPLE} is absorbance of the sample containing blood solution, and A_{NC} and A_{PC} are absorbance of the blood solution in 10 mL of 0.9% NaCl solution and 10 mL of DI water without the sample, respectively. The test was repeated three times, and the average values with standard deviations are presented.

In the blood clotting analysis, 100 µL, 2.5 mg/mL concentration of Arg-based CDs was placed into tubes and incubated at 37 °C in a shaking water bath. Separately, 0.81 mL of the blood in the hemogram tube was reacted with 0.064 mL of 0.2 M CaCl_2 solution, and 0.27 mL of this solution was dropped in the CD-containing tubes. The tubes were incubated at 37 °C in a shaking water bath. After 10 min, 10 mL of DI water was slowly added into the tubes and centrifuged at 100× g for 1 min. The supernatant of this solution was diluted with 40 mL of DI water and measured with a UV-vis spectrophotometer at 542 nm. Blood clotting index of the CDs was examined according to Equation (2):

$$\text{Blood clotting index} = (A_{\text{SAMPLE}}/A_{\text{BLOOD}}) \times 100 \quad (2)$$

where A_{SAMPLE} is absorbance value of the sample interacted with the blood solution, and A_{BLOOD} is absorbance value of the 0.25 mL blood solution in 50 mL DI water. The test was repeated three times, and the average values with standard deviations are presented.

3.5. Cytotoxicity of Arg-Based CDs

The cytotoxicity analyses of Arg CDs were carried out on L929 fibroblast cells. Briefly, 1×10^4 cells were placed into each well of a 96-well plate containing DMEM medium and incubated for 24 h in a 5% CO_2 /95% air atmosphere at 37 °C. At the end of 24 h, the attachment of cells to the well plate surface was checked, the media was removed, and the suspension of the Arg-based CDs in DMEM prepared at 50–1000 µg/mL concentrations were added to the wells. The well plate was incubated for 24 h in a 5% CO_2 /95% air atmosphere at 37 °C. Following the incubation period, the culture media were decanted, and the wells were washed with PBS three times. Then, 100 µL of MTT solution prepared at 0.5 mg/mL concentration was added into the wells, and the plate was incubated at 37 °C for 2 h in dark conditions. The MTT solution was removed, and 200 µL of dimethyl sulfoxide was added to dissolve formazan crystals. Cell viability was determined by measuring the absorbance of the 96-well plate with a plate reader (Multiskan Sky, Thermo, Waltham, MA, USA) at 590 nm. The tests were repeated three times.

3.6. Antimicrobial Activities of Arg CDs and Their Modified Forms

The antimicrobial properties of Arg CDs and their modified forms were determined by microtiter broth dilution methods against gram-negative *Escherichia coli* ATCC 8739 and gram-positive *Staphylococcus aureus* ATCC 6538.

To determine minimum inhibition concentration (MIC) values, overnight bacteria cultures in nutrient broth were diluted to a McFarland standard of 0.5. In short, 100 μL of liquid growth media was added to each well on a 96-well plate. As antibacterial material, 50 mg of Arg-based CDs were suspended in 1 mL 0.9% NaCl solution to prepare a 50 mg/mL initial concentration. Then, 100 μL of this solution was added to the first wells of the 96-well plate and diluted with the existing liquid growth media to obtain concentrations from 0.02 to 25 mg/mL. Then, 5 μL of stock bacteria suspension was added to each well and the 96-well plate was incubated at 37 °C for 24 h incubation time. Minimum inhibition concentration (MIC) was determined as the minimum concentration of antimicrobial material at which no turbidity (visible growth) was observed. The tests were repeated three times, and the average values with standard deviations are presented.

3.7. Photodynamic Antibacterial Activity of Arg-Based CDs

Arg-based CDs were used to determine the photodynamic antibacterial activity under UV light. Briefly, 50 mg/mL concentration of Arg, Arg-EDA, Arg-PEHA, and Arg-PEI CD suspensions were prepared in 0.9% NaCl solution and 20, 100, and 200 μL of these suspensions were dispersed in 1 mL of bacteria solution in 0.9% NaCl solution which contained McFarland 0.5 bacteria colony. Only 1 mL of bacteria solution in 0.9% NaCl solution was used as a control group. These tubes were kept in the dark or under a UV lamp (315–400 nm, UVa, 300 W, Ostram GmbH, Ultra vitalux, Munich, Germany) for 30 min. At 5 min and 30 min, 100 μL of the samples were separately taken and inoculated onto nutrient agar. The plates were kept in a 37 °C incubator for 24 h. At the end of 24 h, bacterial growth and spread in the media were compared with the control group and bacteria cell viability % was noted. The tests were repeated three times, and the average values with standard deviations are presented.

4. Conclusions

Arg CDs prepared via a microwave-assisted method in 2 min were found to be in the 1–10 nm size range with a graphitic structure as determined by TEM images and DLS measurement. The amine modification of Arg CDs as Arg-EDA, Arg-PEHA, and Arg-PEI CDs were successfully achieved using ECH as a coupling agent between the modifying agent and the Arg CDs to enhance their antibacterial properties. The highest zeta potential value was determined for the Arg-PEI CDs with $+34.4 \pm 4.1$ mV. The Arg CDs and Arg-EDA CDs at a 0.25 mg/mL concentration were found to be blood-compatible biomaterials for potential intravenous applications, with a low hemolysis ratio and high blood clotting index. On the other hand, at this concentration, the Arg-PEHA and Arg-PEI CDs were not found to be safe for intravenous administration because of clotting effects within 10 min. However, these materials can potentially be used to stop bleeding as a blood-clotting material in the treatment of certain diseases. Furthermore, all types of Arg-based CDs were non-toxic on L929 fibroblast cells after 24 h incubation at 100 $\mu\text{g}/\text{mL}$ concentration. Interestingly, the antibacterial effect of the Arg CDs was significantly enhanced for the modified form, and the highest antibacterial susceptibility was determined for the Arg-PEI CDs against *E. coli* and *S. aureus* bacteria with a 0.2 mg/mL MIC value. Finally, at 5 mg/mL the fluorescent Arg CDs showed excellent photodynamic activity with 50% bacterial inhibition of *E. coli* under UV light irradiation for 5 min. This photoinduced bacterial growth inhibition was further improved using highly fluorescent Arg-EDA CDs at only 1 mg/mL concentration with almost 80% bacterial inhibition under 30 min UV light irradiation. Therefore, these fluorescent CDs have great potential to be employed in photodynamic therapy to clean or disinfect chronic wounds and scars and might have a wide range of application in the food and beverage industries as packing materials as well as medical textile utilizations.

Author Contributions: Conceptualization, N.S.; methodology, S.S.S., M.S., A.S.Y. and N.S.; validation, S.S.S., M.S. and A.S.Y.; formal analysis, S.S.S., M.S., A.S.Y. and N.S.; investigation, S.S.S., M.S., A.S.Y., R.S.A. and N.S.; resources, R.S.A. and N.S.; data curation, S.S.S., M.S., A.S.Y. and N.S.; writing—original draft preparation, S.S.S., M.S. and A.S.Y.; writing—review and editing, R.S.A. and

N.S.; visualization, R.S.A. and N.S.; supervision, R.S.A. and N.S.; project administration, R.S.A. and N.S.; funding acquisition, R.S.A. and N.S. All authors have read and agreed to the published version of the manuscript.

Funding: This research received no external funding.

Data Availability Statement: The data presented in this study are available on request from the corresponding author.

Acknowledgments: The Scientific Research Commission of Canakkale Onsekiz Mart University FIA-2022-3667 is greatly acknowledged.

Conflicts of Interest: The authors declare no conflict of interest.

References

1. Kang, Z.; Lee, S.-T. Carbon dots: Advances in nanocarbon applications. *Nanoscale* **2019**, *11*, 19214–19224. [[CrossRef](#)]
2. Mishra, V.; Patil, A.; Thakur, S.; Kesharwani, P. Carbon dots: Emerging theranostic nanoarchitectures. *Drug Discov. Today* **2018**, *23*, 1219–1232. [[CrossRef](#)]
3. Ogi, T.; Aishima, K.; Permatasari, F.A.; Iskandar, F.; Tanabe, E.; Okuyama, K. Kinetics of nitrogen-doped carbon dot formation: Via hydrothermal synthesis. *New J. Chem.* **2016**, *40*, 5555–5561. [[CrossRef](#)]
4. Kaczmarek, A.; Hoffman, J.; Morgiel, J.; Mościcki, T.; Stobiński, L.; Szymański, Z.; Małolepszy, A. Luminescent carbon dots synthesized by the laser ablation of graphite in polyethylenimine and ethylenediamine. *Materials* **2021**, *14*, 729. [[CrossRef](#)]
5. Xu, J.; Cui, K.; Gong, T.; Zhang, J.; Zhai, Z.; Hou, L.; Zaman, F.U.; Yuan, C. Ultrasonic-Assisted Synthesis of N-Doped, Multicolor Carbon Dots toward Fluorescent Inks, Fluorescence Sensors, and Logic Gate Operations. *Nanomaterials* **2022**, *12*, 312. [[CrossRef](#)]
6. Lee, Y.S.; Hu, C.C.; Chiu, T.C. Electrochemical synthesis of fluorescent carbon dots for the selective detection of chlortetracycline. *J. Environ. Chem. Eng.* **2022**, *10*, 107413. [[CrossRef](#)]
7. Zhu, H.; Wang, X.; Li, Y.; Wang, Z.; Yang, F.; Yang, X. Microwave synthesis of fluorescent carbon nanoparticles with electrochemiluminescence properties. *Chem. Commun.* **2009**, *34*, 5118–5120. [[CrossRef](#)]
8. Wang, X.; Qu, K.; Xu, B.; Ren, J.; Qu, X. Microwave assisted one-step green synthesis of cell-permeable multicolor photoluminescent carbon dots without surface passivation reagents. *J. Mater. Chem.* **2011**, *21*, 2445–2450. [[CrossRef](#)]
9. Azam, N.; Najabat Ali, M.; Javaid Khan, T. Carbon Quantum Dots for Biomedical Applications: Review and Analysis. *Front. Mater.* **2021**, *8*, 700403. [[CrossRef](#)]
10. Ou, S.F.; Zheng, Y.Y.; Lee, S.J.; Chen, S.T.; Wu, C.H.; Te Hsieh, C.; Juang, R.S.; Peng, P.Z.; Hsueh, Y.H. N-doped carbon quantum dots as fluorescent bioimaging agents. *Crystals* **2021**, *11*, 789. [[CrossRef](#)]
11. Agrawal, N.; Bhagel, D.; Mishra, P.; Prasad, D.; Kohli, E. Post-synthetic modification of graphene quantum dots bestows enhanced biosensing and antibiofilm ability: Efficiency facet. *RSC Adv.* **2022**, *12*, 12310–12320. [[CrossRef](#)] [[PubMed](#)]
12. Juzenas, P.; Chen, W.; Sun, Y.-P.; Coelho, M.A.N.; Generalov, R.; Generalova, N.; Christensen, I.L. Quantum dots and nanoparticles for photodynamic and radiation therapies of cancer. *Adv. Drug Deliv. Rev.* **2008**, *60*, 1600–1614. [[CrossRef](#)] [[PubMed](#)]
13. Li, P.; Liu, S.; Cao, W.; Zhang, G.; Yang, X.; Gong, X.; Xing, X. Low-toxicity carbon quantum dots derived from gentamicin sulfate to combat antibiotic resistance and eradicate mature biofilms. *Chem. Commun.* **2020**, *56*, 2316–2319. [[CrossRef](#)] [[PubMed](#)]
14. Dou, Q.; Fang, X.; Jiang, S.; Chee, P.L.; Lee, T.C.; Loh, X.J. Multi-functional fluorescent carbon dots with antibacterial and gene delivery properties. *RSC Adv.* **2015**, *5*, 46817–46822. [[CrossRef](#)]
15. Wu, X.; Xu, M.; Wang, S.; Abbas, K.; Huang, X.; Zhang, R.; Tedesco, A.C.; Bi, H. F,N-Doped carbon dots as efficient Type I photosensitizers for photodynamic therapy. *Dalt. Trans.* **2022**, *51*, 2296–2303. [[CrossRef](#)]
16. Wang, B.; Cai, H.; Waterhouse, G.I.N.; Qu, X.; Yang, B.; Lu, S. Carbon Dots in Bioimaging, Biosensing and Therapeutics: A Comprehensive Review. *Small Sci.* **2022**, *2*, 2200012. [[CrossRef](#)]
17. Yang, J.; Chen, W.; Liu, X.; Zhang, Y.; Bai, Y. Hydrothermal synthesis and photoluminescent mechanistic investigation of highly fluorescent nitrogen doped carbon dots from amino acids. *Mater. Res. Bull.* **2017**, *89*, 26–32. [[CrossRef](#)]
18. Pei, S.; Zhang, J.; Gao, M.; Wu, D.; Yang, Y.; Liu, R. A facile hydrothermal approach towards photoluminescent carbon dots from amino acids. *J. Colloid Interface Sci.* **2015**, *439*, 129–133. [[CrossRef](#)]
19. Arias Velasco, V.; Caicedo Chacón, W.D.; Carvajal Soto, A.M.; Ayala Valencia, G.; Granada Echeverri, J.C.; Agudelo Henao, A.C. Carbon Quantum Dots Based on Carbohydrates as Nano Sensors for Food Quality and Safety. *Starch/Staerke* **2021**, *73*, 2100044. [[CrossRef](#)]
20. Shaikh, A.F.; Tamboli, M.S.; Patil, R.H.; Bhan, A.; Ambekar, J.D.; Kale, B.B. Bioinspired Carbon Quantum Dots: An Antibiofilm Agents. *J. Nanosci. Nanotechnol.* **2018**, *19*, 2339–2345. [[CrossRef](#)]
21. Yan, H.; Zhang, B.; Zhang, Y.; Su, R.; Li, P.; Su, W. Fluorescent Carbon Dot-Curcumin Nanocomposites for Remarkable Antibacterial Activity with Synergistic Photodynamic and Photothermal Abilities. *ACS Appl. Bio Mater.* **2021**, *4*, 6703–6718. [[CrossRef](#)] [[PubMed](#)]
22. Wu, X.; Abbas, K.; Yang, Y.; Li, Z.; Tedesco, A.C.; Bi, H. Photodynamic Anti-Bacteria by Carbon Dots and Their Nano-Composites. *Pharmaceuticals* **2022**, *15*, 487. [[CrossRef](#)] [[PubMed](#)]

23. Nie, X.; Wu, S.; Mensah, A.; Lu, K.; Wei, Q. Carbon quantum dots embedded electrospun nanofibers for efficient antibacterial photodynamic inactivation. *Mater. Sci. Eng. C* **2020**, *108*, 110377. [[CrossRef](#)] [[PubMed](#)]
24. Marković, Z.M.; Kováčová, M.; Humpolček, P.; Budimir, M.D.; Vajdák, J.; Kubát, P.; Mičušík, M.; Švajdlenková, H.; Danko, M.; Capáková, Z.; et al. Antibacterial photodynamic activity of carbon quantum dots/polydimethylsiloxane nanocomposites against *Staphylococcus aureus*, *Escherichia coli* and *Klebsiella pneumoniae*. *Photodiagnosis Photodyn. Ther.* **2019**, *26*, 342–349. [[CrossRef](#)]
25. Liu, D.; Yang, M.; Liu, X.; Yu, W. Zinc-Doped Carbon Dots as Effective Blue-Light-Activated Antibacterial Agent. *Nano* **2021**, *16*, 2150031. [[CrossRef](#)]
26. Liu, B.; Su, Y.; Wu, S.; Shen, J. Local photothermal/photodynamic synergistic antibacterial therapy based on two-dimensional BP@CQDs triggered by single NIR light source. *Photodiagnosis Photodyn. Ther.* **2022**, *39*, 102905. [[CrossRef](#)]
27. Meziani, M.J.; Dong, X.; Zhu, L.; Jones, L.P.; LeCroy, G.E.; Yang, F.; Wang, S.; Wang, P.; Zhao, Y.; Yang, L.; et al. Visible-Light-Activated Bactericidal Functions of Carbon “Quantum” Dots. *ACS Appl. Mater. Interfaces* **2016**, *8*, 10761–10766. [[CrossRef](#)]
28. Luo, P.G.; Sahu, S.; Yang, S.T.; Sonkar, S.K.; Wang, J.; Wang, H.; Lecroy, G.E.; Cao, L.; Sun, Y.P. Carbon “quantum” dots for optical bioimaging. *J. Mater. Chem. B* **2013**, *1*, 2116–2127. [[CrossRef](#)]
29. Fernando, K.A.S.; Sahu, S.; Liu, Y.; Lewis, W.K.; Gulians, E.A.; Jafariyan, A.; Wang, P.; Bunker, C.E.; Sun, Y.P. Carbon quantum dots and applications in photocatalytic energy conversion. *ACS Appl. Mater. Interfaces* **2015**, *7*, 8363–8376. [[CrossRef](#)]
30. Al Awak, M.M.; Wang, P.; Wang, S.; Tang, Y.; Sun, Y.-P.; Yang, L. Correlation of carbon dots’ light-activated antimicrobial activities and fluorescence quantum yield. *RSC Adv.* **2017**, *7*, 30177–30184. [[CrossRef](#)]
31. Ristic, B.Z.; Milenkovic, M.M.; Dakic, I.R.; Todorovic-Markovic, B.M.; Milosavljevic, M.S.; Budimir, M.D.; Paunovic, V.G.; Dramicanin, M.D.; Markovic, Z.M.; Trajkovic, V.S. Photodynamic antibacterial effect of graphene quantum dots. *Biomaterials* **2014**, *35*, 4428–4435. [[CrossRef](#)] [[PubMed](#)]
32. Brkić, S. Optical Properties of Quantum Dots. *Eur. Int. J. Sci. Technol.* **2016**, *5*, 98–107.
33. Dong, X.; Bond, A.E.; Pan, N.; Coleman, M.; Tang, Y.; Sun, Y.-P.; Yang, L. Synergistic photoactivated antimicrobial effects of carbon dots combined with dye photosensitizers. *Int. J. Nanomed.* **2018**, *13*, 8025–8035. [[CrossRef](#)] [[PubMed](#)]
34. Anand, A.; Unnikrishnan, B.; Wei, S.-C.; Chou, C.P.; Zhang, L.-Z.; Huang, C.-C. Graphene oxide and carbon dots as broad-spectrum antimicrobial agents—A minireview. *Nanoscale Horiz.* **2019**, *4*, 117–137. [[CrossRef](#)]
35. Romero, M.P.; Alves, F.; Stringasci, M.D.; Buzzá, H.H.; Ciol, H.; Inada, N.M.; Bagnato, V.S. One-Pot Microwave-Assisted Synthesis of Carbon Dots and in vivo and in vitro Antimicrobial Photodynamic Applications. *Front. Microbiol.* **2021**, *12*, 1455. [[CrossRef](#)] [[PubMed](#)]
36. Dong, X.; Liang, W.; Meziani, M.J.; Sun, Y.-P.; Yang, L. Carbon Dots as Potent Antimicrobial Agents. *Theranostics* **2020**, *10*, 671–686. [[CrossRef](#)]
37. Abu Rabe, D.I.; Al Awak, M.M.; Yang, F.; Okonjo, P.A.; Dong, X.; Teisl, L.R.; Wang, P.; Tang, Y.; Pan, N.; Sun, Y.P.; et al. The dominant role of surface functionalization in carbon dots’ photo-activated antibacterial activity. *Int. J. Nanomed.* **2019**, *14*, 2655–2665. [[CrossRef](#)]
38. Pandey, R.R.; Chusuei, C.C. Carbon Nanotubes, Graphene, and Carbon Dots as Electrochemical Biosensing Composites. *Molecules* **2021**, *26*, 6674. [[CrossRef](#)]
39. Alavi, M.; Jabari, E.; Jabbari, E. Functionalized carbon-based nanomaterials and quantum dots with antibacterial activity: A review. *Expert Rev. Anti. Infect. Ther.* **2021**, *19*, 35–44. [[CrossRef](#)]
40. Sahiner, N.; Suner, S.S.; Sahiner, M.; Silan, C. Nitrogen and Sulfur Doped Carbon Dots from Amino Acids for Potential Biomedical Applications. *J. Fluoresc.* **2019**, *29*, 1191–1200. [[CrossRef](#)]
41. Suner, S.S.; Sahiner, M.; Ayyala, R.S.; Bhethanabotla, V.R.; Sahiner, N. Nitrogen-Doped Arginine Carbon Dots and Its Metal Nanoparticle Composites as Antibacterial Agent. *C—J. Carbon Res.* **2020**, *6*, 58. [[CrossRef](#)]
42. Khoobi, M.; Delshad, T.M.; Vosooghi, M.; Alipour, M.; Hamadi, H.; Alipour, E.; Hamedani, M.P.; Sadat Ebrahimi, S.E.; Safaei, Z.; Foroumadi, A.; et al. Polyethyleneimine-modified superparamagnetic Fe₃O₄ nanoparticles: An efficient, reusable and water tolerance nanocatalyst. *J. Magn. Magn. Mater.* **2015**, *375*, 217–226. [[CrossRef](#)]
43. Dong, X.; Al Awak, M.; Tomlinson, N.; Tang, Y.; Sun, Y.-P.; Yang, L. Antibacterial effects of carbon dots in combination with other antimicrobial reagents. *PLoS ONE* **2017**, *12*, e0185324. [[CrossRef](#)]
44. Nichols, F.; Chen, S. Graphene Oxide Quantum Dot-Based Functional Nanomaterials for Effective Antimicrobial Applications. *Chem. Rec.* **2020**, *20*, 1505–1515. [[CrossRef](#)]